



Light-Switchable N-Alkylation Using Amine-Functionalized MOF

Yu Huang ^{a,b,c}, Yaru Li ^{d,e,*}, Dongsheng Zhang ^{b,c}, Yuanqiang Mai ^b, Flemming Besenbacher ^f, Chuan Dong ^a, Federico Rosei ^g, Yong Yang ^{c,e}, Yongwang Li ^{c,e}, Hans Niemantsverdriet ^{c,h}, Wenting Liang ^{a,***}, Ren Su ^{b,c,***}

^a Institute of Environmental Science, Shanxi University, Taiyuan 030006, China

^b Soochow Institute for Energy and Materials Innovations (SIEMIS), Suzhou 215006, China

^c SynCat@Beijing, Synfuels China Technology Co. Ltd., Huairou, Beijing 101407, China

^d Tianjian Laboratory of Advanced Biomedical Sciences, Academy of Medical Sciences, Zhengzhou University, Zhengzhou, Henan 450001, China

^e State Key Laboratory of Coal Conversion, Institute of Coal Chemistry, Taiyuan 030001, China

^f Interdisciplinary Nanoscience Center, Aarhus University, Gustav Wieds Vej 14, Aarhus DK-8000, Denmark

^g Department of Chemical and Pharmaceutical Sciences, University of Trieste, Via Giorgieri 1, Trieste 34127, Italy

^h Syngaschem BV, Nuenen 5672 XD, the Netherlands



ARTICLE INFO

Keywords:

Heterogeneous catalysis

Photocatalysis

N-alkylation

Selective C-N cross coupling

Metal organic frameworks

ABSTRACT

Catalytic N-alkylation is a frequently employed method to synthesize secondary amines and imines, yet selectivity control remains as a challenge that normally requires specialized catalysts under harsh reaction conditions. Here we propose a light-switchable N-alkylation of amines with aromatic halides for selective synthesis of secondary amines and imines, using an amine-functionalized metal-organic framework (MIL-125-NH₂) under mild conditions. The MIL-125-NH₂ catalyst possesses Lewis acidic sites, which catalyze direct dehalogenative condensation of bromides with primary amines to produce secondary amines in the dark. Upon irradiation, the MIL-125-NH₂ reduces molecular oxygen to create oxygen radicals, converting bromides into the corresponding aldehydes to yield imines *via* a dehydrative coupling with amines. With appropriate acidity, rapid oxygen reduction kinetics, and optimized adsorption of aromatic bromides and generated water, the system catalyzes the conversion of a wide range of substrates, thus featuring it a promising method for applications.

1. Introduction

N-alkylation of amines represents a direct, atom-economic approach to produce secondary amines, imines, and their derivates, which are important chemicals for life sciences, pharmaceuticals, and the chemical industry in general [1–5]. Multiple synthetic methods to this end have been extensively studied to improve selectivities and expand the substrate scopes under mild reaction conditions [1,6]. Classic synthesis of secondary amines can be realized by nucleophilic substitution, Buchwald–Hartwig and Ullmann condensation, and hydroamination under basic conditions [6–9], though overalkylation of the amine products needs to be avoided [10,11]. Conventional synthesis of imines includes condensation of ketones/alcohols with amines and dehydrogenation of amines using specially designed catalysts and dehydrating

agents [1,12,13]. Since the conversion between secondary amines and the corresponding imines is an easy process, precise control of the N-alkylation to the desired amines and imines remains a challenge.

Homo- and heterogeneous catalytic routes have been studied intensively to achieve selectivity control in N-alkylation for the synthesis of secondary amines and imines *via* the acceptorless dehydrogenative coupling (ADC) and borrowing hydrogen (BH) process (Scheme 1A) [14–16]. Transition metal complexes and nanoparticles (i.e., Pt, Ni, Co) are often employed as catalysts under basic conditions at elevated temperatures to realize controlled N-alkylation [17–22], yet fine tweaking of reaction conditions, product separation and high stability of the catalysts are needed and remain a challenge. Photocatalysis offers an alternative approach for controllable N-alkylation under mild conditions (Scheme 1B) [23,24]. Traxler *et al.* used an acridine-based covalent

* Corresponding author at: Tianjian Laboratory of Advanced Biomedical Sciences, Academy of Medical Sciences, Zhengzhou University, Zhengzhou, Henan 450001, China.

** Corresponding author.

*** Corresponding author at: Soochow Institute for Energy and Materials Innovations (SIEMIS), Soochow University, Suzhou 215006, China.

E-mail addresses: lyr@zzu.edu.cn (Y. Li), liangwt@sxu.edu.cn (W. Liang), suren@suda.edu.cn (R. Su).

organic framework (COF) as photocatalyst for the cross coupling of halides with pyrrolidine under visible light, with NiBr_2 as the promoter (Scheme 1B, upper part) [23]. The COF improves the separation of generated charge carriers to accelerate the debromination of halide molecules, resulting in efficient cross coupling of pyrrolidine with a series of halides to the corresponding secondary amines with high yields. Very recently, Lv *et al.* show that precise synthesis of secondary amines and imines can be realized by simply tuning the identity of metal cocatalyst supported on TiO_2 (Scheme 1B, lower part) [24]. While Fe promotes mild activation of the alcohol molecule for direct condensation to yield secondary amines, the presence of Rh enhances the oxidation power of TiO_2 to produce imines *via* the formation of aldehydes. Though a broad substrate scope is a significant advance of this method, the requirement of metal cocatalysts and the need of UV light limit its application at large scale.

Ideally, a system that enables switchable synthesis of secondary amines and imines by simply tuning the reaction conditions and using one simple catalyst would be preferred. For the cross coupling of aniline with halides, the formation of secondary amines only needs a one-step dehalogenative condensation, whereas the synthesis of imines requires an oxidative dehalogenation and a consecutive dehydrative coupling process. This implies that a dual function catalyst that possesses dehalogenation and oxidation characteristics should work. Apparently, a photocatalyst with surface acidity could be a rational solution to promote the dehalogenative condensation under dark conditions and the oxidative dehalogenation upon irradiation. Additionally, the catalyst should exhibit appropriate adsorption of the halides, a rapid oxygen reduction rate, and a weak adsorption of the generated water molecules. Considering all these criteria, metal organic frameworks (MOFs) may provide a suitable platform for this task, as the metal clusters and the organic linkers offer rich physicochemical properties for catalytic organic transformations [25–32].

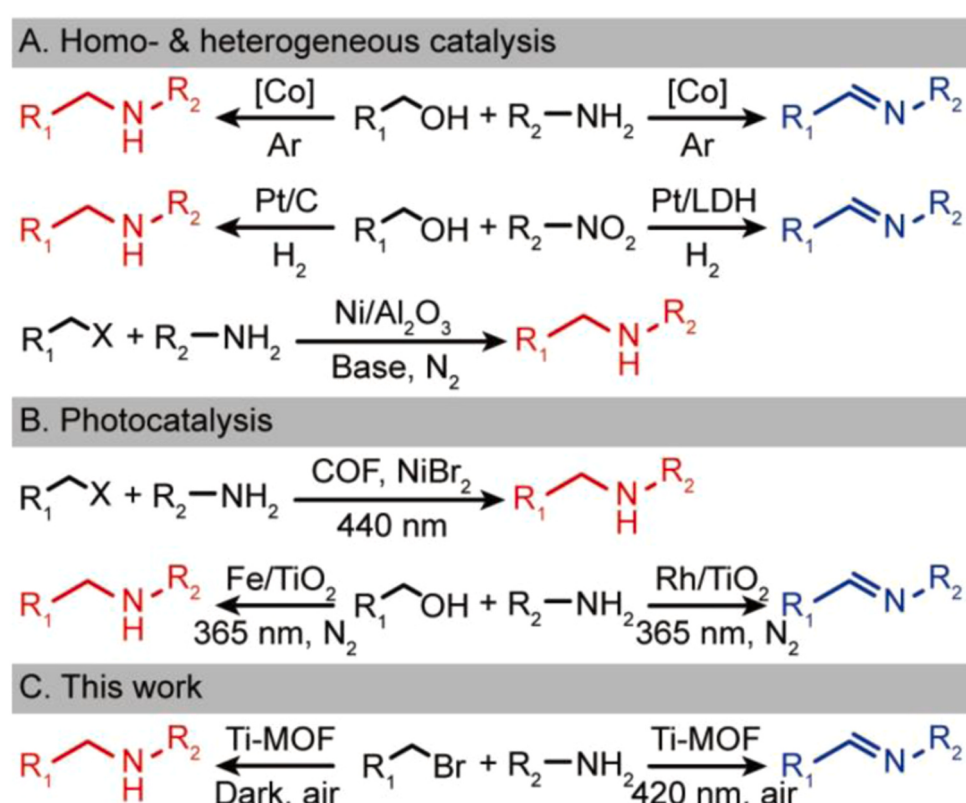
Herein, we report an amine-functionalized Ti-MOF (MIL-125-NH₂) for light-switchable N-alkylation of primary amines with aromatic

halides to synthesize secondary amines and imines selectively under ambient conditions (Scheme 1C). While the Lewis acidic sites on MIL-125-NH₂ promote direct dehalogenative cross coupling to produce secondary amines in the dark, the photogenerated oxygen radicals by MIL-125-NH₂ lead to the oxidative dehalogenation of halides to produce the corresponding ketones and the consecutive dehydrative coupling to yield imines under irradiation. The light switchable N-alkylation of primary amines with halides using MIL-125-NH₂ in terms of reaction rates, reaction pathways, and substrate scope are reported.

2. Experimental section

2.1. Chemicals & synthesis of photocatalysts

All chemicals are analytical grade and were used without further purification. The MIL-125 (Ti) was synthesized by a solvothermal method using terephthalic acid (H₂BDC) as the organic linker [33]. H₂BDC (1.0 g) and tetra-n-butyl titanate (Ti(OC₄H₉)₄, 0.52 mL) were added into a solution containing dimethylformamide (DMF, 18.0 mL) and methanol (MeOH, 2.0 mL). The mixture was stirred for 30 min at room temperature (RT) and then was transferred to a 100 mL Teflon lined autoclave and heated at 150 °C for 24 h. The MIL-125-NH₂ was synthesized using a similar method with some modifications [34,35]. The 2-aminoterephthalic acid (NH₂-H₂BDC, 1.3 g) was chosen as the linker and was dispersed in a 25.0 mL of 1:1 (v/v) mixture of DMF and MeOH. Then 0.52 mL of Ti(OC₄H₉)₄ was added into the solution and stirred for 30 min at RT, which was transferred to a 100 mL Teflon lined autoclave and kept in an oven at 150 °C for 24 h. The MIL-125-OH and MIL-125-NO₂ were prepared using the same method as MIL-125-NH₂, except using 2-hydroxyterephthalic acid and 2-nitroterephthalic acid as organic linkers. The final products were isolated by centrifugation, washed with DMF and MeOH for three times, and dried under vacuum for 12 h at 80 °C.



Scheme 1. Catalytic N-Alkylation of anilines for the synthesis of imines and secondary amines.

2.2. Characterization

X-ray diffraction (XRD) patterns were recorded on a Bruker D8 Advance diffractometer. Fourier transform infrared spectra (FT-IR) were measured using a Bruker VERTEX 70 spectrometer. ^1H and ^{13}C solid state nuclear magnetic resonance (ssNMR) spectra were recorded using an AVANCE III HD-600 MHz spectrometer. The chemical composition and oxidation state of the elements in the catalyst were characterized with an X-ray photoelectron spectrometer equipped with an Al K α X-ray source (XPS, K-Alpha, Thermo Fisher Scientific). Optical properties of the photocatalysts were determined using a photospectrometer (UH4150, Hitachi). The morphology of samples was studied with a scanning electron microscope (SEM, FEI Quanta 400 F) and a

transmission electron microscope (TEM, Titan Themis Cubed G2 300). N_2 adsorption-desorption isotherms were obtained with a physisorption analyzer (Micromeritics, ASAP 2420). Thermogravimetric analysis (TGA) was performed under a flowing nitrogen atmosphere (TA Instruments SDT650).

2.3. Performance evaluation & mechanistic analysis

The photochemical reactions were carried out in a multichannel reactor (SUNCAT INSTRUMENTS). The products were determined by gas chromatography (GC, Agilent GC 6890) and combined gas chromatography and mass spectrometry (GC-MS, Agilent GC 7890 GC system coupled with 5973 network mass selective detector). Product yields

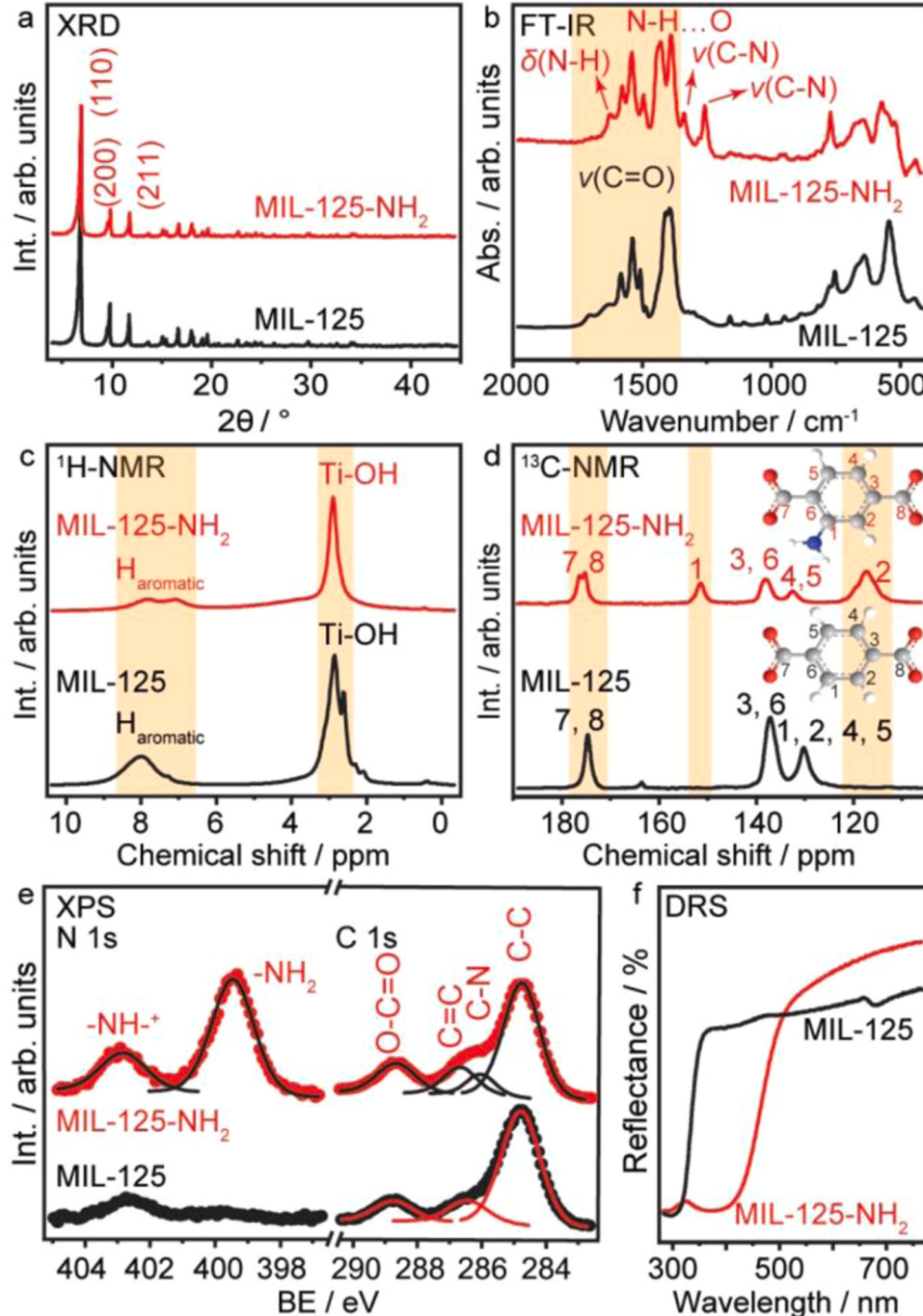


Fig. 1. Characterization of the catalysts. (a)-(f) XRD patterns, FTIR, ssNMR, XPS, and DRS of the as-synthesized MIL-125 and MIL-125-NH₂.

were determined by GC, equipped with an HP-5 MS column and an FID detector. Typical reactions were carried out with 10 mg of catalyst, 8 mM benzyl bromides and 32 mM anilines in 2 mL n-hexane solution at room temperature for 12 h, either in the dark or under 420 nm irradiation for 12 h (30 mW·cm⁻²). All reactions were carried out in air.

The concentration of Br⁻ was analyzed by ion chromatograph (IC, Dionex Aquion). The desorption of ammonia, benzyl bromide, aniline and water from the different catalysts was studied with a chemisorption analyzer (AutoChem II) coupled with a mass spectrometer (MS, OmniStar GSD, Pfeiffer). The evolution of molecular oxygen was followed by a quadrupole mass spectrometer (QMS, HPR-20, Hiden) equipped with an *in-situ* reactor. Radical species were analyzed by electron paramagnetic resonance (EPR) using an X-band JES-X320 spectrometer in the range of 321–331 mT at RT, using a modulation width of 0.1 mT and an amplitude of 400.

3. Results and discussion

3.1. Characterization of the photocatalysts

The amine-functionalized MIL-125 (Ti) MOF (MIL-125-NH₂) is synthesized *via* a classical solvothermal method using tetrabutyl titanate [Ti(OC₄H₉)₄] and 2-amino-benzene-1,4-dicarboxylate as precursors in a 1:1 v/v ratio in a dimethylformamide (DMF)-methanol solution under 150 °C for 24 h (Note S1) [34,35]. For comparison, pristine, hydroxyl-, and nitro- functionalized MIL-125 MOFs have been also synthesized under similar reaction conditions (Note S1) [33,36]. Powder X-ray diffraction (XRD) patterns reveal the successful synthesis of crystalline MIL-125 and its derivatives (Fig. 1a) [33,37,38]. The presence of -NH₂ functional group in the linker barely influences the structure of pristine MIL-125. Fourier transform infrared (FT-IR) adsorption spectroscopy is employed to further study the -NH₂ functionalized MOFs (Fig. 1b). While the pristine MIL-125 shows characteristic symmetrical stretching vibrational peaks of the carboxylate groups (ν [C=O] 1750–1380 cm⁻¹) [39,40], the MIL-125-NH₂ exhibits additional vibrational peaks that can be assigned to δ [N-H] (1625 cm⁻¹) and ν [C-N] (1338 cm⁻¹, 1257 cm⁻¹), indicating the -NH₂ functionalization of the MIL-125 [39, 41]. In addition, the splitting of the peak at ~1400 cm⁻¹ is a clear indication of intermolecular hydrogen bonding between the -NH₂ functional group of one unit cell and a carboxylate group of another unit cell (N-H···O) in MIL-125-NH₂ [42]. Solid state nuclear magnetic resonance (ssNMR) further confirms the successful amination of MIL-125 (Fig. 1c, 1d). The ¹³C spectra reveal that the carbon skeleton of the MOF remains after amine functionalization. Remarkably, a new peak at 151 ppm appears, characteristic of the C-N bond of the 2-amino-benzene-1,4-dicarboxylate linker [43].

X-ray photoelectron spectroscopy (XPS) further confirms the successful amino functionalization of the MIL-125, as evident by substantial peaks characteristic of -NH₂ (399.4 eV) and NH⁺ species (402.8 eV, Fig. 1e) [35,44]. In addition, the deconvoluted C1s spectra reveal the presence of C-N bond (286.1 eV) in MIL-125-NH₂ [40], confirming that the amino group binds to the carbon atom of the linker. Meanwhile, the O1s and Ti2p spectra of the MIL-125-NH₂ remain unchanged compared to those of the pristine MIL-125 (Fig. S1) [40,45]. The symmetric Ti2p peaks at 458.8 eV (Ti2p3/2) and 464.5 eV (Ti2p1/2) confirm the oxidation states of titanium to be 4+ for the titanium-oxo cluster [46, 47]. Diffuse reflectance spectra (DRS) show that the functionalized MIL-125-NH₂ displays visible light absorption up to 500 nm with a bright yellow appearance (Fig. 1f and Fig. S2). In comparison, the pristine MIL-125 only absorbs UV light up to 325 nm. The N₂ adsorption isotherms reveal that the -NH₂ functionalized MIL-125 has a somewhat reduced specific surface area (1060 m² g⁻¹) compared to the pristine MIL-125 (1309 m² g⁻¹), but it still provides sufficient active sites for the sorption of reactants (Fig. S3).

3.2. Photocatalytic performance

We have evaluated different catalysts for the N-alkylation of aniline (32 mM) with benzyl bromide (8 mM) under dark and irradiation under ambient conditions (Fig. 2a). The concentrations of aniline and benzyl bromide are optimized to avoid unwanted byproduct formation caused by polymerization of aniline under irradiation (Fig. S4). While secondary amine (N-benzylaniline, **1a**) *via* dehalogenative condensation is the major product under dark conditions, N-benzylideneaniline (**2a**) is produced *via* a dehydrogenative process upon irradiation. All MIL-125 based catalysts outperform pristine TiO₂ and graphitic carbon nitride (gCN), with MIL-125-NH₂ showing the optimal performance with a complete conversion of benzyl bromide and high selectivity to **1a**. The catalytic performance of TiO₂ remains poor even by extending the reaction time from 12 to 24 h (Table S1). Interestingly, a similar trend is observed for the synthesis of **2a** under irradiation, featuring MIL-125-NH₂ as optimal catalyst. This suggests that selective synthesis of **1a** and **2a** can be simply manipulated by switching the light off or on when using the MIL-125-NH₂ catalyst. Pristine MIL-125 yields less **2a** under 365 nm irradiation, possibly because of poor light absorption in the visible region. No reaction occurs in the absence of a catalyst (Entries 9 and 15, Table S1).

Time courses of photo-switchable N-alkylation of aniline with benzyl bromide using MIL-125-NH₂ catalyst are determined under ambient conditions (Fig. 2b and 2c). In the dark (Fig. 2b), the consumption of benzyl bromide follows first order reaction kinetics ($k=0.65\text{ h}^{-1}$) and reaches a high conversion in 12 h (94%). **1a** is the dominant product over the entire course with a high selectivity (>95%), indicating that **1a** forms by a direct dehalogenative coupling (DDC) path. Upon irradiation (Fig. 2c), a faster conversion of benzyl bromide is observed ($k=0.86\text{ h}^{-1}$). Noticeably, **1a** is the main species in the early stage of the reaction (<1 h); it gradually converts to **2a** upon prolonging the irradiation time. This indicates that **2a** can either be produced directly, or indirectly *via* dehydrogenation of **1a** (Fig. S5), which will be discussed later. The selective synthesis of **1a** and **2a** is maintained even at higher initial concentrations of benzyl bromide (8, 20, and 40 mM) by increasing the reaction time (12, 24, and 36 h, Figs. 2d and 2e), which is of potential interest for practical applications. The C-balances for the synthesis of secondary amine and imine are both ~80%. Additionally, our photo-switchable N-alkylation process shows a high yield (>90%) for both secondary amines and imines, which is comparable with other catalytic approaches for N-alkylation as reported previously (Table S3).

The stability of the MIL-125-NH₂ catalyst has been explored in consideration of practical applications (Fig. 3). A durable performance for four consecutive cycles without noticeable reduction in activity and selectivity is observed under both dark and irradiation conditions, demonstrating a high stability of the MIL-125-NH₂ catalyst for selective synthesis of secondary amines and imines (Fig. 3a and 3d). Additionally, characterizations of the spent catalyst confirms that there is no obvious change after long-term operations (Fig. 3b, 3c, 3e, and 3f). Note that a careful washing after each cycle is key to remove reactants and products in the pore structure of the MOF, and is essential for achieving stable performance. Here DMF and methanol washing was employed after the synthesis of **1a** in the dark, whereas N-methylpyrrolidone and methanol washing was used after the synthesis of **2a** under irradiation.

3.3. Substrate Scope

Table 1 summarizes the general applicability of the MIL-125-NH₂ catalyst for light switchable catalytic N-alkylation of a series of amines with aromatic halides (Figs. S6–S31). All aniline and benzyl bromide derivatives exhibit excellent conversion and selectivity for the synthesis of the corresponding secondary amines (**1a** to **1j**) in the dark. The presence of electron donating groups (EDG) and electron withdrawing group (EWG) on aniline shows a negligible effect on the synthesis of the corresponding secondary amines (**1a**–**1c**). The presence of EDG (p-

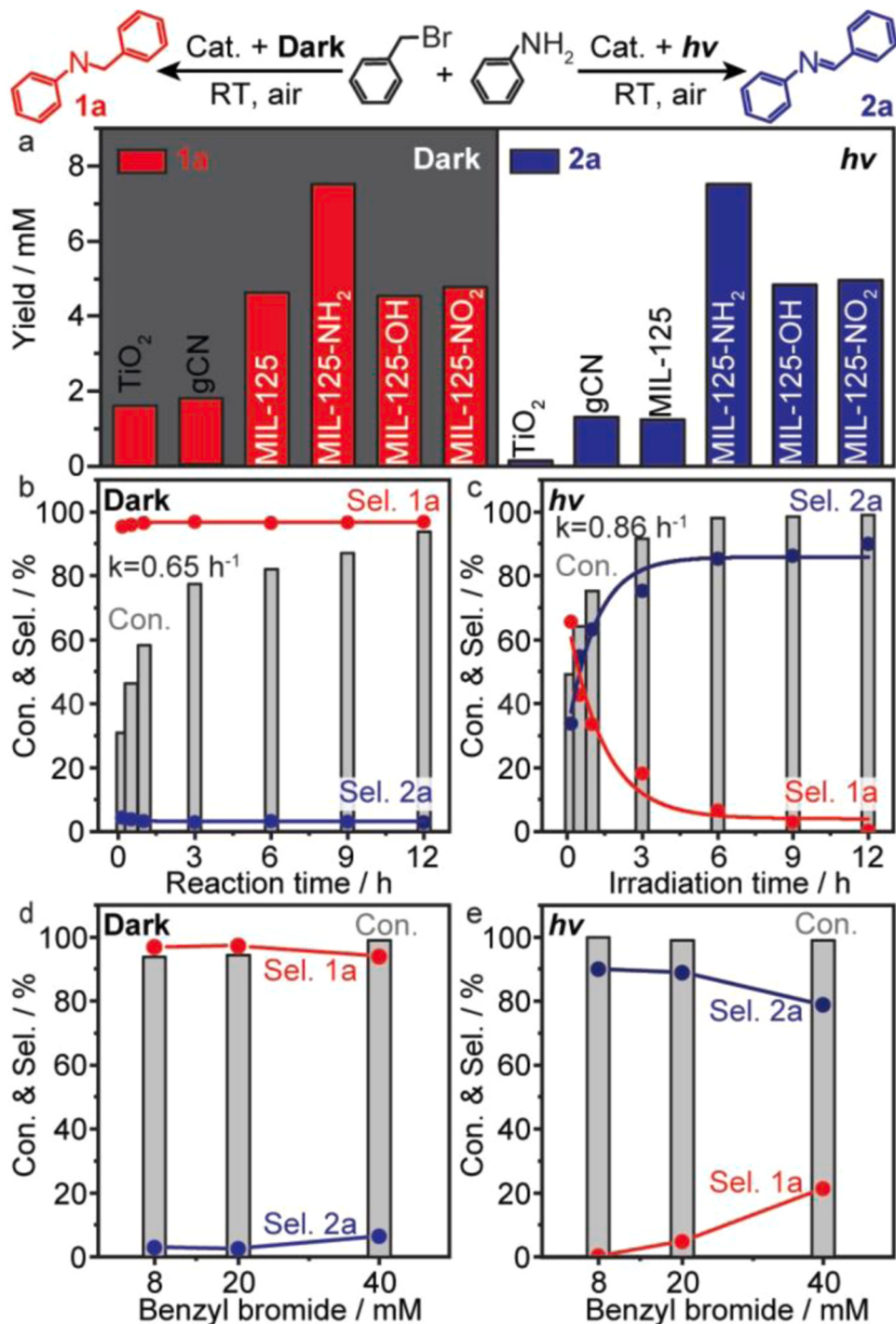


Fig. 2. Switchable catalytic N-alkylation of aniline with benzyl bromide under dark and irradiation at ambient conditions. (a) Comparison of different catalysts for the selective synthesis of N-benzylaniline (**1a**) under dark (left) and the synthesis of N-Benzylideneaniline (**2a**) under irradiation (right). Reaction conditions: 12 h of reaction time; 10 mg photocatalysts in 2 mL n-hexane solution with 8 mM benzyl bromide and 32 mM aniline. A 420 nm LED (30 mW·cm⁻²) is used for gCN and functionalized MIL-125, and a 365 nm LED (14 mW·cm⁻²) is used for TiO₂ and MIL-125. (b) and (c) Time course of **1a** and **2a** evolution under dark and upon irradiation using MIL-125-NH₂. (d) and (e) Effect of starting concentrations of benzyl bromide and aniline under dark and upon irradiation. The ratio of [benzyl bromide]/[aniline] is fixed at 1:4. Conversion (Con.) and selectivity (Sel.) are determined by GC.

methyl) or EWG (*p*-bromo, *o*-cholo) on benzyl bromide does not significantly influence conversion and selectivity (**1d**–**1j**). Remarkably, a high conversion and selectivity are also achieved when an aliphatic amine (butylamine) is employed (**1k**). In addition, the N-alkylation of aniline with *p*-chloro-benzyl chloride and *m*-methoxy-benzyl chloride into N-[(*p*-chlorophenyl)methyl]aniline (**1l**) and N-(*m*-methoxybenzyl)aniline (**1m**) can also be realized with high conversion and selectivity,

respectively. Similarly, both aniline and benzyl bromide derivatives show high conversion and selectivity for the synthesis of the corresponding imines (**2a** to **2k**) under irradiation, regardless of the presence of electron donating or withdrawing groups. Cross-coupling of *p*-bromo- and *o*-cholo-benzyl bromides with some aniline derivatives shows a slightly reduced selectivity (**2h** and **2j**) to imines. Nevertheless, the cross coupling of aliphatic amine with benzyl bromide also shows favorable

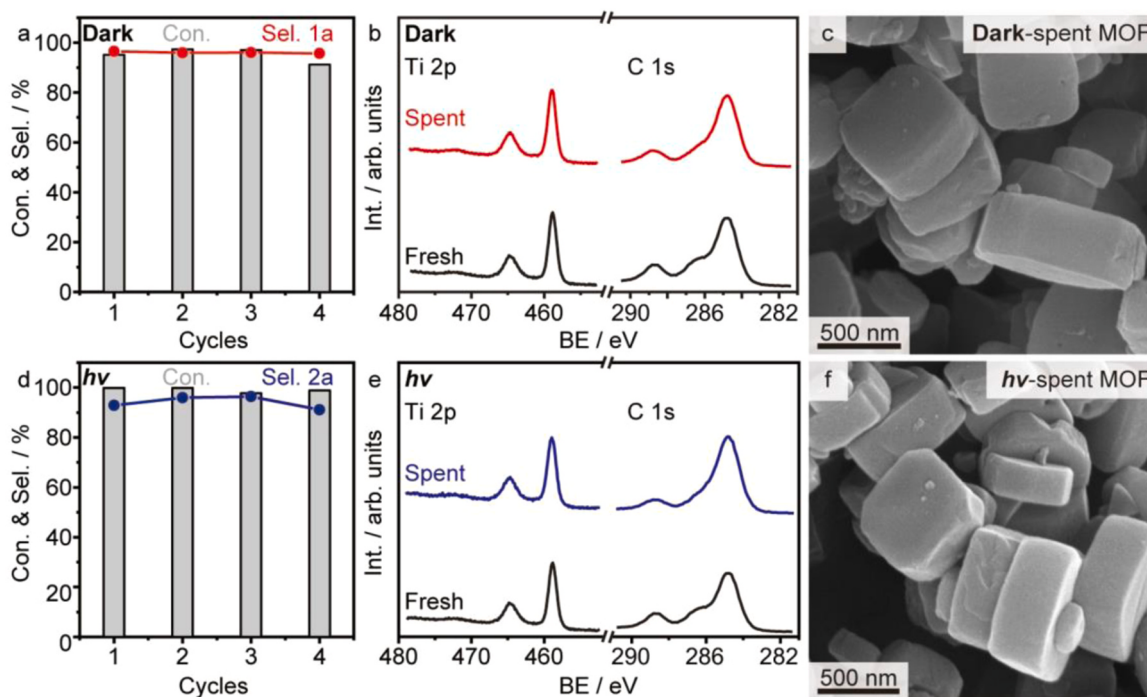


Fig. 3. Stability of the MIL-125-NH₂ catalyst. (a)-(c) Recycle test for the synthesis of **1a** under dark and characterizations of the spent catalyst by XPS and SEM. Reaction conditions: 18 h of reaction time, 10 mg catalysts in 2 mL n-hexane solution with 8 mM benzyl bromide and 32 mM aniline. The catalyst powders were collected and rinsed by DMF and MeOH prior to each run. (d)-(f) Recycle test for the synthesis of **2a** under irradiation and characterizations of the spent catalyst by XPS and SEM. Reaction conditions: 18 h of irradiation time (420 nm LED, 30 mW·cm⁻¹), 10 mg catalysts in 2 mL n-hexane solution with 8 mM benzyl bromide and 32 mM aniline. The catalyst powders were collected and rinsed by N-methylpyrrolidone and MeOH prior to each run.

Table 1
Substrate scope for light switchable N-alkylation of anilines with benzyl halides using MIL-125-NH₂.

	Dark		$h\nu$	
	RT, air	R ¹ -NH ₂ + X-	RT, air	$h\nu$
Dark^[a]				
	R ¹ =H: 1a , Con. 94%; Sel. 97%			R ¹ =H: 2a , Con. 99%; Sel. 91%
	m-Et: 1b , Con. 99%; Sel. 99%			m-Et: 2b , Con. 95%; Sel. 89%
	m-Cl: 1c , Con. 99%; Sel. 99%			m-Cl: 2c , Con. 98%; Sel. 90%
	R ¹ =H: 1d , Con. 99%; Sel. 99%			R ¹ =H: 2d , Con. 85%; Sel. 99%
	m-Et: 1e , Con. 81%; Sel. 99%			m-Et: 2e , Con. 88%; Sel. 82%
	m-Cl: 1f , Con. 99%; Sel. 99%			m-Cl: 2f , Con. 99%; Sel. 84%
	R ¹ =H: 1g , Con. 99%; Sel. 99%			R ¹ =H: 2g , Con. 93%; Sel. 86%
	m-Et: 1h , Con. 90%; Sel. 99%			m-Et: 2h , Con. 82%; Sel. 62%
	m-Cl: 1i , Con. 85%; Sel. 99%			m-Cl: 2i , Con. 77%; Sel. 89%
	R ¹ =H: 1j , Con. 92%; Sel. 99%			2j , Con. 85%; Sel. 75%
		1k, Con. 99%; Sel. 99%		2k , Con. 74%; Sel. 72%
		R ¹ =H: 1l , Con. 83%; Sel. 91%		2l , Con. 98%; Sel. 98%
		R ¹ =H: 1m , Con. 91%; Sel. 95%		2m , Con. 99%; Sel. 99%

conversion and selectivity to the corresponding imine (**2k**). We have further examined the synthesis of imines employing two representative benzyl chlorides, both of which are fully converted into the corresponding 1-(4-chlorophenyl)-N-phenyl-methanamine (**2l**) and N-phenyl-3-methoxybenzylideneamine (**2m**) with high selectivity, indicating the

capabilities of light-switchable N-alkylation with a wide range of halides.

Reaction conditions: [a] 10 mg catalyst, 8 mM benzyl halide and 32 mM aniline in 2 mL n-hexane solution under dark conditions at RT for 10 h; [b] dark for 12 h; [c] 20 mg catalyst, under dark conditions for

48 h; [d] under 420 nm irradiation for 10 h ($30 \text{ mW}\cdot\text{cm}^{-2}$); [e] under 420 nm irradiation for 12 h; [f] under 420 nm irradiation for 15 h; [g] 20 mg catalyst, under 420 nm irradiation for 48 h; all reactions in air.

3.4. Reaction mechanisms

MIL-125-NH₂ promotes the N-alkylation of aniline with benzyl bromide owing to its superior debromination activity, both under dark and irradiation conditions, as quantitatively analyzed by ion chromatography (IC) of the evolved Br⁻ anions (Figs. 4a, 4b, and S32, Note S2). An immediate decrease of benzyl bromide is observed in the dark, which is accompanied by the formation of Br⁻ with a similar rate constant (0.02 min^{-1} , Fig. 4a). The total Br concentration remains constant for the entire reaction. The debromination of benzyl bromide and the evolution of Br⁻ anions is slightly accelerated by 420 nm irradiation (0.03 min^{-1} , Fig. 4b). In comparison, no evolution of Br⁻ anions is observed for pristine TiO₂ under either condition (Fig. S33). These results indicate that the MIL-125-NH₂ is a dual functional catalyst that exhibits both acid catalytic and photocatalytic properties.

The reaction pathways have further been investigated by stepwise dosing of benzyl bromide and aniline into the catalyst-hexane suspension under dark and irradiation conditions (Figs. 4c and 4d). A significant adsorption of benzyl bromide on the MIL-125-NH₂ occurs in the first 4 h under dark conditions (Fig. 4c). In contrast, both MIL-125 and

TiO₂ show a negligible adsorption of benzyl bromide (Fig. S34). This is possibly due to halogen bonding between benzyl bromide and the linker of MIL-125-NH₂ [48–51]. Upon dosing aniline (32 mM) after 4 h, **1a** forms immediately as the dominant product for the entire experiment. Upon irradiation, benzyl bromide rapidly converts to benzaldehyde rapidly within the first 4 h on MIL-125-NH₂ (Fig. 4d). A consecutive dosing of aniline results in the formation of **2a**, and a complete depletion of generated benzaldehyde within 1 h of irradiation. This suggests that the formation of **2a** undergoes an acceptorless dehydrogenative coupling (ADC) process with the formation of water as byproduct. In contrast, neither pristine MIL-125 nor TiO₂ generate benzaldehyde or **2a** as the final product (Fig. S34), revealing the dual function of the MIL-125-NH₂ catalyst in accelerating oxidative debromination of benzyl bromide and dehydrogenative coupling between benzaldehyde and aniline. This may relate to the adsorption and mild activation of benzyl bromide on MIL-125-NH₂, as will be discussed subsequently.

The unique catalytic behavior of the MIL-125-NH₂ is assigned to the acidic surface properties combined with optimized redox kinetics for generating radical species (Fig. 5). Temperature programmed desorption of ammonia (NH₃-TPD) shows two distinctive desorption peaks at 130 and 300 °C for both pristine MIL-125 and MIL-125-NH₂ (Fig. 5a, Note S3), which correspond to weak and medium acidity of the MOF catalysts originating from the undercoordinated Ti sites [52–55]. The comparable intensity of the low temperature desorption peak (~120 °C)

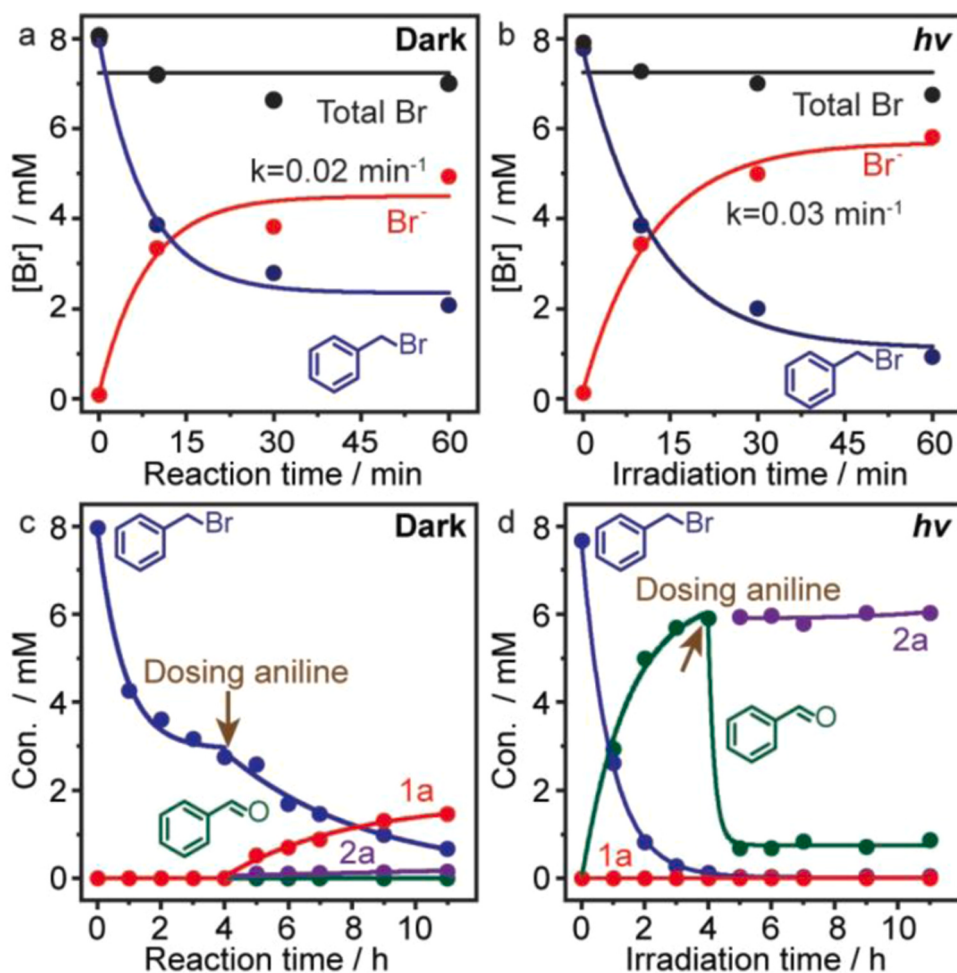


Fig. 4. Reaction mechanisms of MIL-125-NH₂ catalyzed switchable N-alkylation. (a) and (b) Evolution of Br species in the dark and under irradiation using MIL-125-NH₂. Reaction conditions: 10 mg photocatalysts in 2 mL n-hexane solution with 8 mM benzyl bromide and 32 mM aniline under air atmosphere at RT, using a 420 nm LED ($30 \text{ mW}\cdot\text{cm}^{-2}$). (c) and (d) Evolution of intermediates and final products during stepwise addition of benzyl bromide and aniline in the dark and under irradiation. Reaction condition: 80 mg of MIL-125-NH₂, 8 mM benzyl bromide in 16 mL n-hexane solution; 35 μL of aniline (32 mM) is added into the system after 4 h.

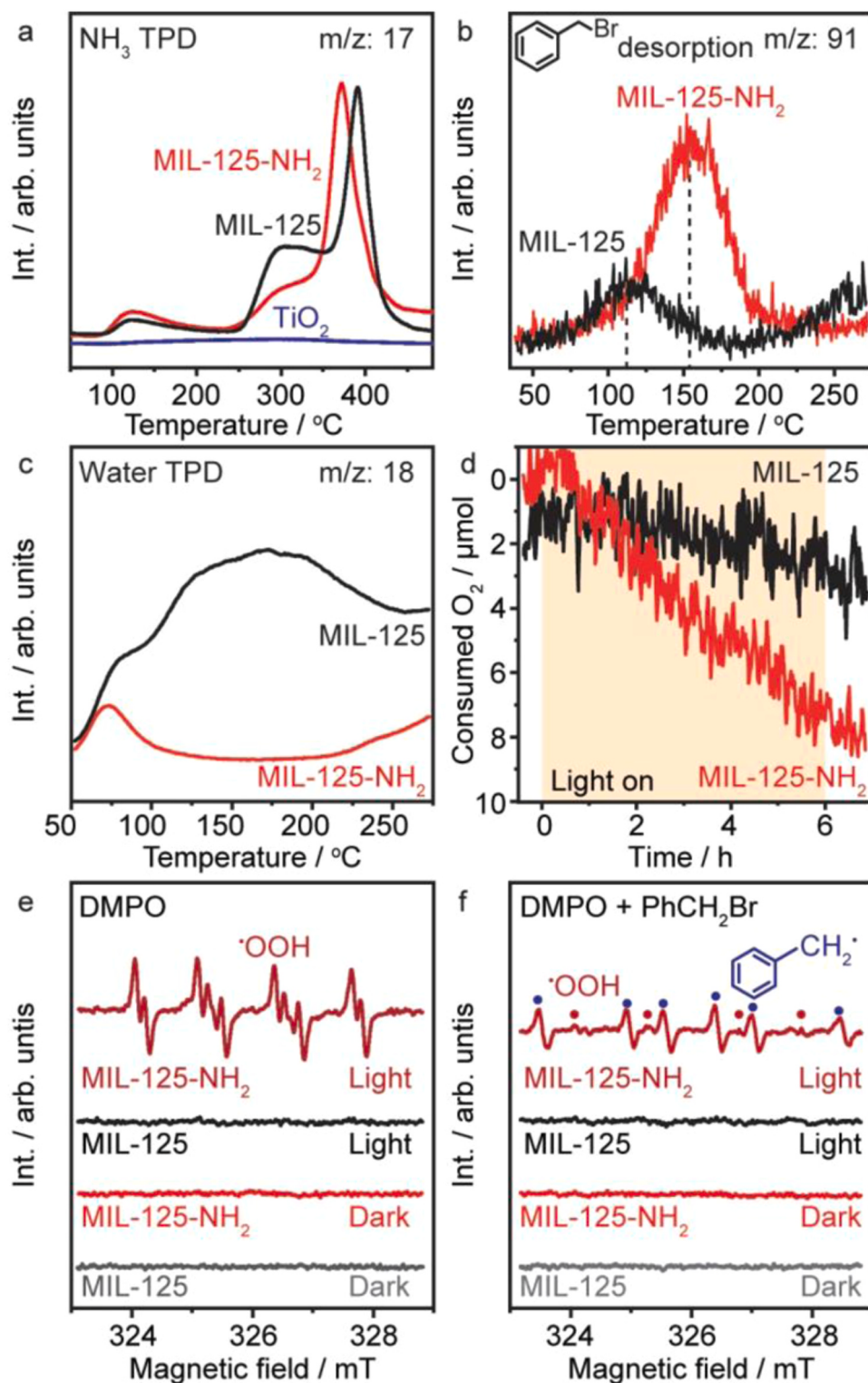


Fig. 5. Promotion mechanisms of MIL-125-NH₂ catalyzed switchable N-alkylation. (a)-(c) TPD of NH₃, benzyl bromide, and water, respectively. (d) *In-situ* MS of photocatalytic oxygen reduction. Reaction conditions: 300 μmol benzyl bromide, 30 mg catalyst, 20 mbar of O₂, 420 nm irradiation (30 mW·cm⁻²) at RT. (e) and (f) Evolution of radical species without and with benzyl bromide in the dark and under irradiation using DMPO as the spin trap. Reaction conditions: 5 mg catalyst, 20 mM benzyl bromide, and 100 mM DMPO in DMSO, irradiated at RT for 1 min.

observed for both samples indicates that the introduction of -NH₂ functional group barely influences the weak acidic sites. The CO₂-TPD shows that the introduction of -NH₂ does not significantly enhance the weak basic sites (Fig. S35). In comparison, a noticeable drop of intensity for the desorption peak at ~300 °C is observed for the MIL-125-NH₂

compared with the pristine MIL-125, implying that the presence of -NH₂ functional group reduces the medium acidic sites of MIL-125. The desorption peaks above 350 °C are caused by the decomposition of the MOFs, which is consistent with the TGA results (Fig. S36)[56]. In comparison, TiO₂ shows only very weak NH₃ adsorption and,

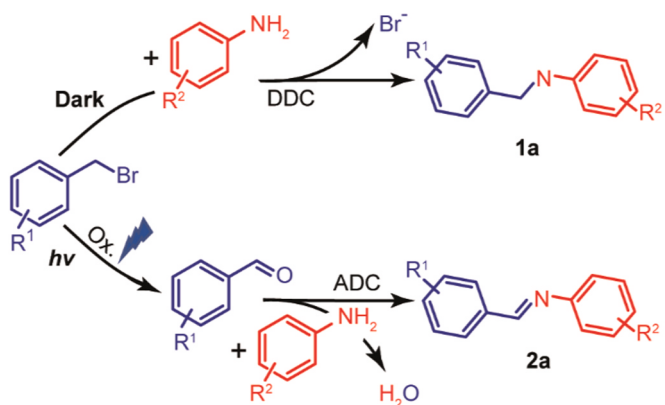
consequently, negligible surface acidity. The adsorption of benzyl bromide and aniline are further analyzed by TPD (Fig. 4b and S37). While a distinct desorption peak of benzyl bromide ($m/z=91$) is observed for the MIL-125-NH₂ at ~ 150 °C, MIL-125 exhibits a very weak desorption peak at 110 °C (Fig. 5b). Both MIL-125 and MIL-125-NH₂ show negligible adsorption of aniline ($m/z=93$, Fig. S37). This indicates that the mild adsorption of benzyl bromide on MIL-125-NH₂ benefits either the acidic or photocatalytic debromination processes, thus enabling its interaction with aniline to produce **1a** or **2a**. In addition, TPD shows that water adsorbs extensively and relatively strong on pristine MIL-125, but substantially less on the MIL-125-NH₂. While the intense desorption peak between 100 and 250 °C for pristine MIL-125 is associated to H₂O interacting with surface sites through hydrogen bonding, the small desorption peak at 72 °C for the MIL-125-NH₂ is attributed to H₂O trapped in the interparticle space [57,58]. This implies that the intermolecular hydrogen bonding between -NH₂ and the -COO reduces the hydrogen bonding sites available for water, thus resulting in a weakened interaction of water with the MOF. Apparently, this weak interaction benefits the rapid depletion of generated water molecules during the ADC process for the synthesis of **2a** under irradiation.

The reduction kinetics of molecular oxygen during photocatalytic debromination of benzyl bromide has been studied by *in-situ* mass spectrometry (MS, Fig. 5d, S38, S39 and S40, Note S4). Here, a low partial pressure of oxygen (20 mbar) is employed for rapid analysis of O₂ consumption. Interestingly, the MIL-125-NH₂ shows a significantly faster oxygen consumption rate (1.2 $\mu\text{mol}\cdot\text{h}^{-1}$) than pristine MIL-125 (0.3 $\mu\text{mol}\cdot\text{h}^{-1}$) under irradiation, which is essential for the N-alkylation of aniline to synthesis **2a** via the ADC step. As expected, the -OH and -NO₂ functionalized MOFs also show a slow oxygen reduction rate ($\sim 0.2 \mu\text{mol}\cdot\text{h}^{-1}$) under irradiation (Fig. S39a). Electron spin resonance (ESR) spectroscopy is performed to identify photogenerated radical species by employing 5,5-dimethyl-1-pyrroline N-oxide (DMPO) as the spin trap in dimethyl sulfoxide (DMSO) solution (Fig. 5f and S39, Note S5). The pristine MIL-125 shows silent spectra under both dark and irradiation conditions (gray and black curve, Fig. 5e), implying the poor photocatalytic performance. In comparison, characteristic resonance peaks that can be assigned to superoxide radicals ($^{\bullet}\text{OOH}$) are observed for MIL-125-NH₂ upon irradiation (Fig. 5e) [59]. Interestingly, the $^{\bullet}\text{OOH}$ signal observed for the MIL-125-NH₂ has almost vanished when benzyl bromide is added into the system, with the appearance of benzyl radical (PhCH_2^{\bullet}) as the major radical species (Fig. 5f) [60]. This indicates that the $^{\bullet}\text{OOH}$ radicals are efficiently used for the oxidative debromination of benzyl bromide. In contrast, while no radical species are detected for MIL-125 regardless of irradiation (Fig. 5f), the MIL-125-OH and MIL-125-NO₂ can generate oxygen radicals but are inefficient in the formation of benzyl radicals (Figs. S39b and S39c). Additionally, the presence of aniline shows a negligible effect on the spectra, confirming that the oxidative dehalogenation is the initial step of the N-alkylation (Fig. S39d). This is also evidenced by the formation of water vapor upon irradiation, confirming the condensation coupling of photogenerated benzaldehyde with aniline to yield **2a** (Fig. S40).

The proposed mechanisms for light-switchable N-alkylation of aniline with benzyl bromide using the MIL-125-NH₂ catalyst are shown in Scheme 2. In the dark, the -NH₂ group in MIL-125-NH₂ enhances the adsorption of benzyl bromide, which reacts with aniline via a direct dehalogenative coupling (DDC) path to yield **1a** on the Lewis acid site that is provided by the Ti-O cluster. Upon irradiation, photogenerated $^{\bullet}\text{OOH}$ radicals attack the surface adsorbed benzyl bromide to yield benzaldehyde, which then reacts with aniline via the acceptorless dehydrogenative coupling (ADC) path to produce **2a**. The weakly adsorbed water molecules are rapidly removed from the surface, thus emptying the active site for the next catalytic cycle.

4. Conclusion

In summary, we propose a light switchable N-alkylation route for



Scheme 2. Proposed mechanisms of light-switchable catalytic N-alkylation of anilines for the synthesis of imines and secondary amines using MIL-125-NH₂. ADC and DDC stand for acceptorless dehydrogenative and direct dehalogenative coupling, respectively.

controllable synthesis of secondary amines and imines using a dual functional MIL-125-NH₂ catalyst. While the Lewis acidic sites on MIL-125-NH₂ boost the direct dehalogenative condensation of benzyl bromides with anilines to generate secondary amines in the dark, irradiation switches the conversion of benzyl bromides to benzyl radicals *via* an oxidative debromination path, resulting in the formation of aldehydes and consequently a dehydrative coupling with aniline to yield imines. The MIL-125-NH₂ exhibits appropriate acidity, fast oxygen reduction kinetics, and an optimized adsorption of benzyl bromides and water molecules, thus leading to optimized catalytic performance under both reaction conditions. Additionally, the light switchable N-alkylation process offers a wide substrate scope, featuring it a promising method for applications, provided a method for large-scale production of the necessary MOF materials becomes available, preferably via a solvent-free process.

CRediT authorship contribution statement

Yu Huang: Writing – original draft, Methodology, Investigation, Formal analysis, Data curation, Conceptualization. **Yaru Li:** Writing – review & editing, Writing – original draft, Visualization, Supervision, Methodology, Investigation, Formal analysis, Data curation, Conceptualization. **Dongsheng Zhang:** Methodology, Investigation, Formal analysis, Data curation, Conceptualization. **Yuanqiang Mai:** Investigation, Formal analysis, Data curation. **Flemming Besenbacher:** Writing – review & editing, Writing – original draft, Supervision, Conceptualization. **Chuan Dong:** Supervision, Conceptualization. **Federico Rosei:** Writing – review & editing, Writing – original draft, Supervision, Funding acquisition. **Yong Yang:** Writing – review & editing, Supervision, Resources, Funding acquisition. **Yongwang Li:** Writing – review & editing, Supervision, Resources, Funding acquisition. **Hans Niemannsverdriet:** Writing – review & editing, Writing – original draft, Supervision, Resources. **Wenting Liang:** Writing – review & editing, Writing – original draft, Supervision, Resources, Methodology, Funding acquisition, Conceptualization. **Ren Su:** Writing – review & editing, Writing – original draft, Validation, Supervision, Resources, Methodology, Investigation, Funding acquisition, Data curation, Conceptualization.

Declaration of Competing Interest

The authors declare that they have no known competing financial interests or personal relationships that could have appeared to influence the work reported in this paper.

Data Availability

Data will be made available on request.

Acknowledgments

RS and WL thank the NSFC (project No.: 21972100, 21976113). RS acknowledges the Project of Innovation and Entrepreneurship of the Jiangsu Province (grant No.: JSSCRC202010539), and the Suzhou Foreign Academician Workstation (project No.: SWY2022001) for financial support. We also acknowledge support from the Soochow Municipal laboratory for low carbon technologies and industries.

Appendix A. Supporting information

Supplementary data associated with this article can be found in the online version at [doi:10.1016/j.apcatb.2024.123924](https://doi.org/10.1016/j.apcatb.2024.123924).

References

- B. Chen, L. Wang, S. Gao, Recent advances in aerobic oxidation of alcohols and amines to imines, *ACS Catal.* 5 (2015) 5851–5876.
- N.W. Dow, A. Cabré, D.W.C. MacMillan, A general N-alkylation platform via copper metallaphotoredox and silyl radical activation of alkyl halides, *Chem* 7 (2021) 1827–1842.
- J.W. Kim, K. Yamaguchi, N. Mizuno, Heterogeneously catalyzed selective N-alkylation of aromatic and heteroaromatic amines with alcohols by a supported ruthenium hydroxide, *J. Catal.* 263 (2009) 205–208.
- C.W. Cheung, X. Hu, Amine synthesis via iron-catalyzed reductive coupling of nitroarenes with alkyl halides, *Nat. Commun.* 7 (2016) 12494–12502.
- R. Mao, A. Frey, J. Balon, X. Hu, Decarboxylative C(sp³)-N cross-coupling via synergistic photoredox and copper catalysis, *Nat. Catal.* 1 (2018) 120–126.
- J. Magano, J.R. Dunetz, Large-scale applications of transition metal-catalyzed couplings for the synthesis of pharmaceuticals, *Chem. Rev.* 111 (2011) 2177–2250.
- F. Monnier, M. Taillefer, Catalytic C-C, C-N, and C-O Ullmann-type coupling reactions, *Angew. Chem. Int. Ed.* 48 (2009) 6954–6971.
- W. Ma, X. Zhang, J. Fan, Y. Liu, W. Tang, D. Xue, C. Li, J. Xiao, C. Wang, Iron-catalyzed anti-markovnikov hydroamination and hydroamidation of allylic alcohols, *J. Am. Chem. Soc.* 141 (2019) 13506–13515.
- F. Niu, Q. Wang, Z. Yan, B.T. Kusema, A.Y. Khodakov, V.V. Ordonsky, Highly efficient and selective N-alkylation of amines with alcohols catalyzed by in situ rehydrated titanium hydroxide, *ACS Catal.* 10 (2020) 3404–3414.
- C. Chiappe, D. Pieraccini, Direct mono-N-alkylation of amines in ionic liquids: chemoselectivity and reactivity, *Green Chem.* 5 (2003) 193–197.
- A.K. Szardenig, T.S. Burkoth, G.C. Loo, D.A. Campbell, A reductive alkylation procedure applicable to both solution- and solid-phase syntheses of secondary amines, *J. Org. Chem.* 61 (1996) 6720–6722.
- C. Gunanathan, D. Milstein, Applications of acceptorless dehydrogenation and related transformations in chemical synthesis, *Science* 341 (2013) 1229712.
- X. Hao, X. Yu, H. Li, Z. Zhang, Y. Wang, J. Li, The preparation of full-range BiOBr/BiOI heterojunctions and the tunability of their photocatalytic performance during the synthesis of imines under visible light irradiation, *Appl. Surf. Sci.* 528 (2020) 147015–147024.
- K. Paudel, S. Xu, O. Hietsoi, B. Pandey, C. Onuh, K. Ding, Switchable imine and amine synthesis catalyzed by a well-defined cobalt complex, *Organometallics* 40 (2021) 418–426.
- X. Han, X. Chen, Y. Zou, S. Zhang, Electronic state regulation of supported Pt catalysts dictates selectivity of imines/secondary amines from the cascade transformation of nitroarenes and aldehydes, *Appl. Catal. B* 268 (2020). No. 118451.
- J.-C. Castillo, J. Orrego-Hernández, J. Portilla, Cs₂CO₃-Promoted direct N-alkylation: highly chemoselective synthesis of N-alkylated benzylamines and anilines, *Eur. J. Org. Chem.* 2016 (2016) 3824–3835.
- S. Huang, Z. Zhao, Z. Wei, M. Wang, Y. Chen, X. Wang, F. Shao, X. Zhong, X. Li, J. Wang, Targeted regulation of the selectivity of cascade synthesis towards imines/secondary amines by carbon-coated Co-based catalysts, *Green Chem.* 24 (2022) 6945–6954.
- X. Zhang, J. Zhao, C. Che, J. Qin, T. Wan, F. Sun, J. Ma, Y. Long, Uniformly microporous diatomite supported Ni^{0/2+} catalyzed controllable selective reductive amination of benzaldehydes to primary amines, secondary imines and secondary amines, *J. Catal.* 416 (2022) 129–138.
- R. Fertig, T. Irrgang, F. Freitag, J. Zander, R. Kempe, Manganese-catalyzed and base-switchable synthesis of amines or imines via borrowing hydrogen or dehydrogenative condensation, *ACS Catal.* 8 (2018) 8525–8530.
- A. Jati, K. Dey, M. Nurhuda, M.A. Addicoat, R. Banerjee, B. Maji, Dual metalation in a two-dimensional covalent organic framework for photocatalytic C-N cross-coupling reactions, *J. Am. Chem. Soc.* 144 (2022) 7822–7833.
- J.J. Chen, J.H. Fang, X.Y. Du, J.Y. Zhang, J.Q. Bian, F.L. Wang, C. Luan, W.L. Liu, J. R. Liu, X.Y. Dong, et al., Enantioconvergent Cu-catalysed N-alkylation of aliphatic amines, *Nature* 618 (2023) 294–300.
- Q. Yang, Q. Wang, Z. Yu, Substitution of alcohols by N-nucleophiles via transition metal-catalyzed dehydrogenation, *Chem. Soc. Rev.* 44 (2015) 2305–2329.
- M. Traxler, S. Gisbertz, P. Pachfule, J. Schmidt, J. Roeser, S. Reischauer, J. Rabeah, B. Pieber, A. Thomas, Acridine-functionalized covalent organic frameworks (COFs) as photocatalysts for metallaphotocatalytic C-N cross-coupling, *Angew. Chem. Int. Ed.* 61 (2022) e202117738.
- D. Lv, Y. Li, W. Qiao, D. Zhang, Y. Mai, N. Cai, H. Xiang, Y. Li, H. Niemantsverdriet, W. Hao, et al., Metal cocatalyst mediated photocatalytic dehydrogenative-condensation and direct condensation cross-coupling of aniline and alcohol, *Appl. Catal. B* 309 (2022). No. 121264.
- Y. Zhang, J.Y. Ying, Main-chain organic frameworks with advanced catalytic functionalities, *ACS Catal.* 5 (2015) 2681–2691.
- J. Liu, L. Chen, H. Cui, J. Zhang, L. Zhang, C.Y. Su, Applications of metal-organic frameworks in heterogeneous supramolecular catalysis, *Chem. Soc. Rev.* 43 (2014) 6011–6061.
- X. Feng, Y. Song, W. Lin, Dimensional reduction of Lewis acidic metal-organic frameworks for multicomponent reactions, *J. Am. Chem. Soc.* 143 (2021) 8184–8192.
- L. Jiao, Y. Wang, H.L. Jiang, Q. Xu, Metal-organic frameworks as platforms for catalytic applications, *Adv. Mater.* 30 (2018) 1703663.
- G. Cai, P. Yan, L. Zhang, H.C. Zhou, H.L. Jiang, Metal-organic framework-based hierarchically porous materials: synthesis and applications, *Chem. Rev.* 121 (2021) 12278–12326.
- Y.B. Huang, J. Liang, X.S. Wang, R. Cao, Multifunctional metal-organic framework catalysts: synergistic catalysis and tandem reactions, *Chem. Soc. Rev.* 46 (2017) 126–157.
- G. Lu, F. Chu, X. Huang, Y. Li, K. Liang, G. Wang, Recent advances in Metal-Organic Frameworks-based materials for photocatalytic selective oxidation, *Coord. Chem. Rev.* 450 (2022) 214240.
- D. Zhao, X. Li, K. Zhang, J. Guo, X. Huang, G. Wang, Recent advances in thermocatalytic hydrogenation of unsaturated organic compounds with metal-organic frameworks-based materials: construction strategies and related mechanisms, *Coord. Chem. Rev.* 487 (2023) 215159.
- Y. Fu, D. Sun, Y. Chen, R. Huang, Z. Ding, X. Fu, Z. Li, An amine-functionalized titanium metal-organic framework photocatalyst with visible-light-induced activity for CO₂ reduction, *Angew. Chem. Int. Ed.* 51 (2012) 3364–3367.
- X.-M. Cheng, X.-Y. Dao, S.-Q. Wang, J. Zhao, W.-Y. Sun, Enhanced photocatalytic CO₂ reduction activity over NH₂-MIL-125(Ti) by facet regulation, *ACS Catal.* 11 (2021) 650–658.
- Y. Isaka, Y. Kawase, Y. Kuwahara, K. Mori, H. Yamashita, Two-phase system utilizing hydrophobic metal-organic frameworks (MOFs) for photocatalytic synthesis of hydrogen peroxide, *Angew. Chem. Int. Ed.* 58 (2019) 5402–5406.
- M. Dan-Hardi, C. Serre, T. Frot, L. Rozes, G. Maurin, C. Sanchez, G. Férey, A new photoactive crystalline highly porous titanium(IV) dicarboxylate, *J. Am. Chem. Soc.* 131 (2009) 10857–10859.
- C. Zhang, C. Xie, Y. Gao, X. Tao, C. Ding, F. Fan, H.L. Jiang, Charge separation by creating band bending in metal-organic frameworks for improved [h]otocatalytic hydrogen evolution, *Angew. Chem. Int. Ed.* 61 (2022) e202204108.
- Z. Wu, X. Huang, H. Zheng, P. Wang, G. Hai, W. Dong, G. Wang, Aromatic heterocycle-grafted NH₂-MIL-125(Ti) via conjugated linker with enhanced photocatalytic activity for selective oxidation of alcohols under visible light, *Appl. Catal. B* 224 (2018) 479–487.
- X. Zhang, K. Yue, R. Rao, J. Chen, Q. Liu, Y. Yang, F. Bi, Y. Wang, J. Xu, N. Liu, Synthesis of acidic MIL-125 from plastic waste: Significant contribution of N orbital for efficient photocatalytic degradation of chlorobenzene and toluene, *Appl. Catal. B* 310 (2022). No. 121300.
- W. Zhang, W. Huang, J. Jin, Y. Gan, S. Zhang, Oxygen-vacancy-mediated energy transfer for singlet oxygen generation by diketone-anchored MIL-125, *Appl. Catal. B* 292 (2021). No. 120197.
- X. Li, K. Zhang, X. Huang, Z. Wu, D. Zhao, G. Wang, Thermo-enhanced photocatalytic oxidation of amines to imines over MIL-125-NH₂@Ag@COF hybrids under visible light, *Nanoscale* 13 (2021) 19671–19681.
- Z.-Q. Bai, L.-Y. Yuan, L. Zhu, Z.-R. Liu, S.-Q. Chu, L.-R. Zheng, J. Zhang, Z.-F. Chai, W.-Q. Shi, Introduction of amino groups into acid-resistant MOFs for enhanced U (VI) sorption, *J. Mater. Chem. A* 3 (2015) 525–534.
- S. Devautour-Vinot, G. Maurin, C. Serre, P. Horcajada, D. Paula da Cunha, V. Guillerm, E. de Souza Costa, F. Taullele, C. Martineau, Structure and dynamics of the functionalized MOF type UiO-66(Zr): NMR and dielectric relaxation spectroscopies coupled with DFT calculations, *Chem. Mater.* 24 (2012) 2168–2177.
- H. Wang, X. Yuan, Y. Wu, G. Zeng, X. Chen, L. Leng, Z. Wu, L. Jiang, H. Li, Facile synthesis of amino-functionalized titanium metal-organic frameworks and their superior visible-light photocatalytic activity for Cr(VI) reduction, *J. Hazard. Mater.* 286 (2015) 187–194.
- F. Guo, M. Yang, R.-X. Li, Z.-Z. He, Y. Wang, W.-Y. Sun, Nanosheet-engineered NH₂-MIL-125 with highly active facets for enhanced solar CO₂ reduction, *ACS Catal.* 12 (2022) 9486–9493.
- X. Huang, X. Li, W. Xia, B. Hu, M. Muhler, B. Peng, Highly dispersed Pd clusters/nanoparticles encapsulated in MOFs via in situ auto-reduction method for aqueous phenol hydrogenation, *J. Mater. Sci. Technol.* 109 (2022) 167–175.
- Y. Li, P. Ren, D. Zhang, W. Qiao, D. Wang, X. Yang, X. Wen, M.H. Rummeli, H. Niemantsverdriet, J.P. Lewis, et al., Rationally designed metal cocatalyst for selective photosynthesis of bibenzyls via dehalogenative C-C homocoupling, *ACS Catal.* 11 (2021) 4338–4348.
- K.E. Riley, P. Hobza, The relative roles of electrostatics and dispersion in the stabilization of halogen bonds, *Phys. Chem. Chem. Phys.* 15 (2013) 17742–17751.

[49] J.P.M. Lommerse, A.J. Stone, R. Taylor, F.H. Allen, The Nature and geometry of intermolecular interactions between halogens and oxygen or nitrogen, *J. Am. Chem. Soc.* 118 (1996) 3108–3116.

[50] C. Gropp, B.L. Quigley, F. Diederich, Molecular recognition with resorcin[4]arene cavitands: switching, halogen-bonded capsules, and enantioselective complexation, *J. Am. Chem. Soc.* 140 (2018) 2705–2717.

[51] D.L. Widner, Q.R. Knauf, M.T. Merucci, T.R. Fritz, J.S. Sauer, E.D. Speetzen, E. Bosch, N.P. Bowling, Intramolecular halogen bonding supported by an aryldiyne linker, *J. Org. Chem.* 79 (2014) 6269–6278.

[52] D. Farrusseng, S. Aguado, C. Pinel, Metal-organic frameworks: opportunities for catalysis, *Angew. Chem. Int. Ed.* 48 (2009) 7502–7513.

[53] G. Ye, Y. Gu, W. Zhou, W. Xu, Y. Sun, Synthesis of defect-rich titanium terephthalate with the assistance of acetic acid for room-temperature oxidative desulfurization of fuel oil, *ACS Catal.* 10 (2020) 2384–2394.

[54] B. Bohigues, S. Rojas-Buzo, M. Moliner, A. Corma, Coordinatively unsaturated Hf-MOF-808 prepared via hydrothermal synthesis as a bifunctional catalyst for the tandem N-alkylation of amines with benzyl alcohol, *ACS Sustain. Chem. Eng.* 9 (2021) 15793–15806.

[55] N.-Y. Topsøe, K. Pedersen, E.G. Derouane, Infrared and temperature-programmed desorption study of the acidic properties of ZSM-5-type zeolites, *J. Catal.* 70 (1981) 41–52.

[56] M. Oveisi, M.A. Asli, N.M. Mahmoodi, MIL-Ti metal-organic frameworks (MOFs) nanomaterials as superior adsorbents: synthesis and ultrasound-aided dye adsorption from multicomponent wastewater systems, *J. Hazard. Mater.* 347 (2018) 123–140.

[57] C. Ma, C. Yang, B. Wang, C. Chen, F. Wang, X. Yao, M. Song, Effects of H₂O on HCHO and CO oxidation at room-temperature catalyzed by MCo₂O₄ (M=Mn, Ce and Cu) materials, *Appl. Catal. B* 254 (2019) 76–85.

[58] Y. Wang, F. Wang, Q. Song, Q. Xin, S. Xu, J. Xu, Heterogeneous ceria catalyst with water-tolerant Lewis acidic sites for one-pot synthesis of 1,3-diols via Prins condensation and hydrolysis reactions, *J. Am. Chem. Soc.* 135 (2013) 1506–1515.

[59] D. Zhang, P. Ren, W. Liu, Y. Li, S. Sallie, F. Han, W. Qiao, Y. Liu, Y. Fan, Y. Cui, et al., Photocatalytic abstraction of hydrogen atoms from water using hydroxylated graphitic carbon nitride for hydrogenative coupling reactions, *Angew. Chem. Int. Ed.* 61 (2022) e202204256.

[60] R. Wang, G. Qiu, Y. Xiao, X. Tao, W. Peng, B. Li, Optimal construction of WO₃-H₂O/Pd/CdS ternary Z-scheme photocatalyst with remarkably enhanced performance for oxidative coupling of benzylamines, *J. Catal.* 374 (2019) 378–390.